Investigating the Goodman Diagram for Short-fibre Carbon Reinforced Polypropylene Composites

P.B.S.Bailey[1], P.R.Wilson[2]

[1] Instron Dynamic Systems, Coronation Road, High Wycombe, HP12 3SY, UK.
peter_bailey@instron.com, http://go.instron.com/fatigue
[2] WMG, University of Warwick, UK, https://www2.warwick.ac.uk/fac/sci/wmg/research/

Keywords: Fatigue, Short fibre, Strain, Thermoplastic

ABSTRACT

The fatigue behaviour of an automotive grade, short fibre reinforced injection moulding compound within a tension-only region of the Goodman diagram [1] was mapped at several frequencies. The effects of strain rate and creep were measured, by testing specimens at different frequencies, Measurements were taken under a variety of loading ratios and mean stress levels, while taking with non-contact measurements of strain and temperature. This paper presents an illustration of how the particular combination of static and dynamic loads significantly affects the long term life expectancy of this type of material, the complexity of developing an effective test program, and how the use of more sophisticate measurements than simply cycles-to-failure can give significantly more insight into material performance.

1 INTRODUCTION

The requirement for reduced vehicle carbon emissions and energy consumption has arrived at the point of being a real and extremely urgent concern, leading automotive manufacturers to pursue the most aggressive weight reduction measures possible. It appears that their goals are only achievable by use of various types composite material and compound structures throughout the vehicle; one aspect of which will be the use of injection moulded polymer matrix composites for semi-structural components (such as engine mounts). While the critical design criterial for much of the body structure centre around crash-worthiness, many other components depend most heavily upon fatigue resistance, since this is what determines the minimum amount of material required for a component to reliably survive for the necessary design-life. Fatigue of continuous-fibre composites has gone through several cycles of research interest already since the early 1980s, and recently more widespread work is taking place on all types of thermoplastic fatigue. However, the need now appears to be to provide material models of comparable clarity and confidence to those available for metals, which can be used in finite element analysis for design.

The Goodman diagram (also known as Haigh or Soderberg diagram [2,3]) was originally a tool in life prediction of metals, to relate the effects of fatigue stress and mean stress. Though some contest its utility for that application, it now offers an interesting avenue of investigation in characterising the fatigue behaviour of composites. It appears likely that it will be particularly relevant to thermoplastic matrices where there is little or no truly linear-elastic region where creep behaviour is expected to play a significant role, although the original metals approach may need significant modifications. A particular example would be the use of short fibre reinforced composites for semi-structural automotive applications, such as those typified by the compound used in this experiment, but industry concerns are also being expressed for continuous fibre reinforced thermoplastics in structural aerospace applications.

2 EXPERIMENTAL

A short carbon fibre reinforced polypropylene injection moulding compound, under development at WMG, was used to manufacture sub-size standard geometry tensile specimens. The material used for this experiment uses a short fibre reinforcement currently under development, and specimens were moulded with an automated miniature injection moulding machine, using a single cavity mould. The specimens were used in the as-moulded condition, having a gauge section of 20mm x 4mm x 1.5mm.

Mechanical tests were performed using an Instron Electropuls 10 kN loadframe with linear electric motor actuator. Direct, non-contact strain measurement was provided by an Instron AVE2 video extensometer, operating in dynamic mode to provide un-filtered data at an acquisition rate of 490Hz. For this test, system data was collected at 1kHz, and the Instron 8800 controlled provides control loop closure at 10kHz. Dynamic mechanical analysis calculations were performed on-line during the test using WaveMatrix test software, removing the need for post-processing and providing live data on a full range of DMA parameters including phase angle, complex-, storage- and loss-modulus.

Monotonic tensile tests were conducted at a number of different test speeds, to determine a characteristic failure stress at a strain rate roughly equivalent to that expected in cyclic loading.
Cyclic tests were conducted in force control, at a frequency of 5Hz, for a range of peak force levels equating to between 0.6x and 1.1x the peak stress determined in monotonic tests, and at loading ratios (R-ratios) of 0, 0.2, 0.4, 0.8, -0.2, and -0.4. Fully reversed and compression-compression tests were not possible with this specimen geometry due to lack of constraint resulting in buckling.

3 RESULTS

3.1 Monotonic tests

Specimens appear to exhibit good repeatability in monotonic tests, as illustrated by the 3 specimens shown in Fig. 1, for 2 mm/s test speed. Peak force was consistently recorded as 43.8 ± 0.2 MPa for the batch of specimens at this speed. A single plot for lower test speed of 0.2 mm/s (a representative quasi-static test speed for thermoplastics) is also shown; it is little surprise that this material shows some strain rate sensitivity in its performance resulting in lower stress and drawing stress.

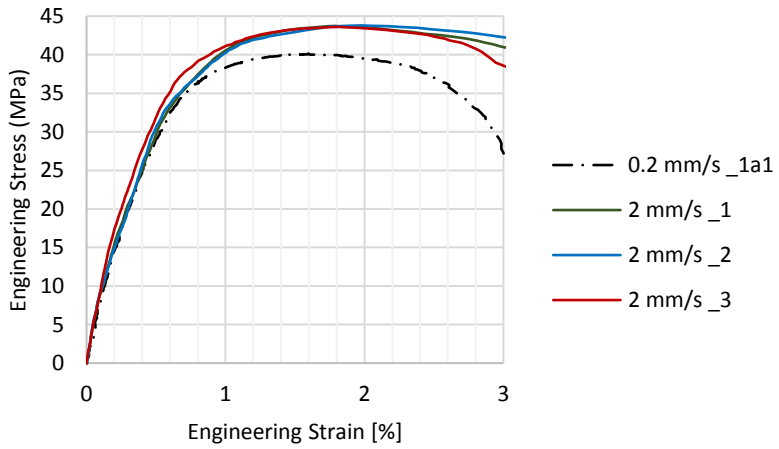

Figure 1: Monotonic tests at 2 mm/s and 0.2 mm/s, plotting engineering stress vs engineering strain

3.2 Fatigue test data

Results are tabulated for respective loading ratio, peak stress, mean stress and stress amplitude in, below. Table 1 shows conventional basic fatigue metrics of cycles to failure. Table 2 shows the resulting strain range and mean, at start of test, half-life, and penultimate full cycle. Table 3 shows dynamic stiffness and loss tangent, also at start of test, half-life, and penultimate full cycle.

Peak stress [MPa]	Loading Ratio	Minimum Stress [MPa]	Mean stress [MPa]	Stress amplitude [MPa]	Cycles to failure
48.4	-0.4	-19.36	14.52	33.88	22
48.4	-0.2	-9.68	19.36	29.04	21
48.4	0	0.00	24.20	24.20	6
48.4	0.2	9.68	29.04	19.36	14
48.4	0.4	19.36	33.88	14.52	9
44	-0.4	-17.60	13.20	30.80	43
44	-0.2	-8.80	17.60	26.40	37
44	0	0.00	22.00	22.00	41
44	0.2	8.80	26.40	17.60	35
44	0.4	17.60	30.80	13.20	24
44	0.8	35.20	39.60	4.40	6
39.6	-0.4	-15.84	11.88	27.72	101
39.6	-0.2	-7.92	15.84	23.76	97
39.6	0	0.00	19.80	19.80	170
39.6	0.2	7.92	23.76	15.84	154
39.6	0.4	15.84	27.72	11.88	99
39.6	0.8	31.68	35.64	3.96	39
37.4	-0.4	-14.96	11.22	26.18	204
37.4	-0.2	-7.48	14.96	22.44	205
37.4	0	0.00	18.70	18.70	575
37.4	0.2	7.48	22.44	14.96	1363
37.4	0.4	14.96	26.18	11.22	507
37.4	0.8	29.92	33.66	3.74	95
35.2	-0.4	-14.08	10.56	24.64	547
35.2	-0.2	-7.04	14.08	21.12	1294
35.2	0	0	17.6	17.60	5437
35.2	0.2	7.04	21.12	14.08	5083
35.2	0.4	14.08	24.64	10.56	1405
35.2	0.8	28.16	31.68	3.52	287
33	0.8	26.4	29.7	3.30	1425
30.8	0.8	24.64	27.72	3.08	6481
26.4	*0.8*	*21.12*	23.76	*2.64*	*80207**
					**no failure*

Table 1: Cycles-to-failure data from fatigue tests

Loading Ratio	Mean stress [MPa]	Stress amplitude [MPa]	Cycles to failure	Cycle 2 strain range [%]	Half-life strain range [%]	Final strain range [%]	Cycle 2 mean strain [%]	Half-life mean strain [%]	Final mean strain [%]
-0.4	14.52	33.88	22	0.723699	1.379733	2.332779	0.289517	0.53646	1.035767
-0.2	19.36	29.04	21	0.683253	1.110424	1.877146	0.408696	0.652267	1.15787
0	24.20	24.20	6	0.741293	0.806663	0.806663	0.424937	0.722065	0.722065
0.2	29.04	19.36	14	0.739479	0.681631	0.86895	0.59289	1.154226	1.606322
0.4	33.88	14.52	9	0.677768	0.516563	0.680355	0.746883	1.428679	2.024012
-0.4	13.20	30.80	43	0.621418	1.452521	3.151207	0.255892	0.552935	1.677376
-0.2	17.60	26.40	37	0.540186	1.147636	2.052332	0.340887	0.612319	1.203371
0	22.00	22.00	41	0.59669	1.05377	1.584849	0.390267	0.88127	1.73449
0.2	26.40	17.60	35	0.516905	0.740177	1.098588	0.445301	1.062438	1.823045
0.4	30.80	13.20	24	0.483612	0.459149	0.687624	0.613324	1.276876	2.053873
0.8	39.60	4.40	6	0.443473	0.361381	0.362308	1.252948	1.643849	1.973825
-0.4	11.88	27.72	101	0.551045	1.435015	2.5623	0.202995	0.520262	1.210453
-0.2	15.84	23.76	97	0.492952	1.181289	1.778993	0.298717	0.601113	1.07971
0	19.80	19.80	170	0.477851	1.074686	1.581025	0.304037	0.906269	1.767315
0.2	23.76	15.84	154	0.392847	0.711627	0.930946	0.35387	0.989289	1.625412
0.4	27.72	11.88	99	0.329669	0.517249	0.671339	0.45775	1.12781	1.851843
-0.4	11.22	26.18	204	0.484163	1.422602	2.397715	0.193749	0.548512	1.185788
-0.2	14.96	22.44	205	0.486328	1.59579	2.642492	0.304878	0.854011	1.786748
0	18.70	18.70	575	0.413408	1.042825	1.389894	0.287025	1.037318	1.843808
0.2	22.44	14.96	1363	0.339244	0.709749	0.999611	0.343401	1.347936	2.740115
0.4	26.18	11.22	507	0.2821	0.4675	0.559215	0.410658	1.291181	2.160008
0.8	33.66	3.74	95	0.142158	0.149647	0.174301	0.686592	1.488516	2.375833
-0.4	10.56	24.64	547	0.495201	1.454705	2.774729	0.180526	0.59752	1.482971
-0.2	14.08	21.12	1294	0.394845	1.252956	2.197175	0.235076	0.781471	1.698977
0	17.60	17.60	5437	0.391217	0.917837	1.233936	0.251012	1.132503	2.099158
0.2	21.12	14.08	5083	0.314732	0.632999	0.804604	0.304527	1.319101	2.546927
0.4	24.64	10.56	1405	0.279337	0.45239	0.495486	0.405067	1.381627	2.124222
0.8	31.68	3.52	287	0.121436	0.12806	0.255982	0.611805	1.523365	2.749485
0.8	29.70	3.30	1425	0.09015	0.123727	0.192205	0.58294	1.739304	3.499383
0.8	27.72	3.08	6481	0.081273	0.135643	0.120195	0.472249	1.650021	2.740761

Table 2: Cyclic strain data during fatigue tests

Loading Ratio	Mean stress [MPa]	Stress amplitude [MPa]	Cycles to failure	Initial tan-δ	Half-life tan-δ	Final tan-δ	Initial dynamic stiffness [MPa]	Half-life dynamic stiffness [MPa]	Final dynamic stiffness [MPa]
-0.4	14.52	33.88	22	0.181119	0.260013	0.418422	5710	4143	2523
-0.2	19.36	29.04	21	0.219379	0.27508	0.450367	5197	3904	2407
0	24.20	24.20	6	0.281602	0.301225		4104	3795	
0.2	29.04	19.36	14	0.340837	0.248501	0.344562	3191	3653	2924
0.4	33.88	14.52	9	0.343318	0.334552	0.401148	3124	3212	2612
-0.4	13.20	30.80	43	0.188465	0.26376	0.571708	6206	3827	1544
-0.2	17.60	26.40	37	0.253862	0.248722	0.822595	5962	4027	1921
0	22.00	22.00	41	0.241861	0.265312	0.413293	4811	3565	2330
0.2	26.40	17.60	35	0.263212	0.231344	0.386263	4233	4081	2747
0.4	30.80	13.20	24	0.316496	0.25329	0.370894	3219	4159	2916
0.8	39.60	4.40	6	0.447474	0.416173		1023	1060	
-0.4	11.88	27.72	101	0.148494	0.233161	0.433735	6521	3826	2024
-0.2	15.84	23.76	97	0.179511	0.232306	0.37061	6381	4125	2646
0	19.80	19.80	170	0.191495	0.259071	0.381677	5392	3611	2417
0.2	23.76	15.84	154	0.194352	0.203887	0.345308	4846	4212	3166
0.4	27.72	11.88	99	0.233963	0.175503	0.348087	4262	4429	3435
0.8	35.64	3.96	39	0.223815	0.190787	0.531742	2589	4748	1925
-0.4	11.22	26.18	204	0.130622	0.246979	0.449928	6937	3671	2040
-0.2	14.96	22.44	205	0.199345	0.27494	0.48312	5287	2700	1513
0	18.70	18.70	575	0.142377	0.230425	0.310856	5888	3597	2633
0.2	22.44	14.96	1363	0.161782	0.184272	0.284095	5493	4157	2955
0.4	26.18	11.22	507	0.204389	0.147524	0.251302	4474	4595	3867
0.8	33.66	3.74	95	0.248798	0.121518	0.226486	2847	4467	4113
-0.4	10.56	24.64	547	0.135877	0.237923	0.507652	6458	3529	1624
-0.2	14.08	21.12	1294	0.12329	0.255873	0.426969	6303	3229	1733
0	17.60	17.60	5437	0.156106	0.185773	0.292428	6286	3886	2793
0.2	21.12	14.08	5083	0.174404	0.156762	0.256054	5762	4384	3457
0.4	24.64	10.56	1405	0.140133	0.151541	0.169436	4978	4709	4226
0.8	31.68	3.52	287	0.150761	0.125706	0.422838	3222	5197	2527
0.8	29.70	3.30	1425	0.108708	0.043515	0.179918	3469	5229	3423
0.8	27.72	3.08	6481	0.075864	0.048833	0.119743	3412	4486	5053

Table 3: Dynamic stiffness and loss tangent data during fatigue tests

Simply plotting the basic data from Table 1, as in Fig. 2, suggests that peak stress can be used with fairly good correlation, to determine a general purpose S-N curve relationship. As would be expected, neither mean stress nor stress amplitude are useful parameters without separating curves for different loading ratio.

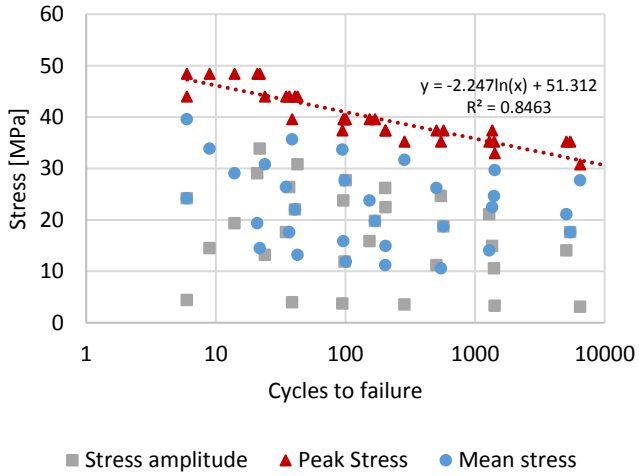

Figure 2: Stress vs cycles to failure (S-N) plot for full dataset

3.3 Fitting of fatigue life data

Separating data by loading ratio means that S-N curves can be plotted and fitted to determine a relationship between stress levels and cycles to failure, as shown in the examples in Fig. 3. Plotting stress against log(cycles) gives a roughly linear relationship, which was fitted for each loading ratio within this dataset.

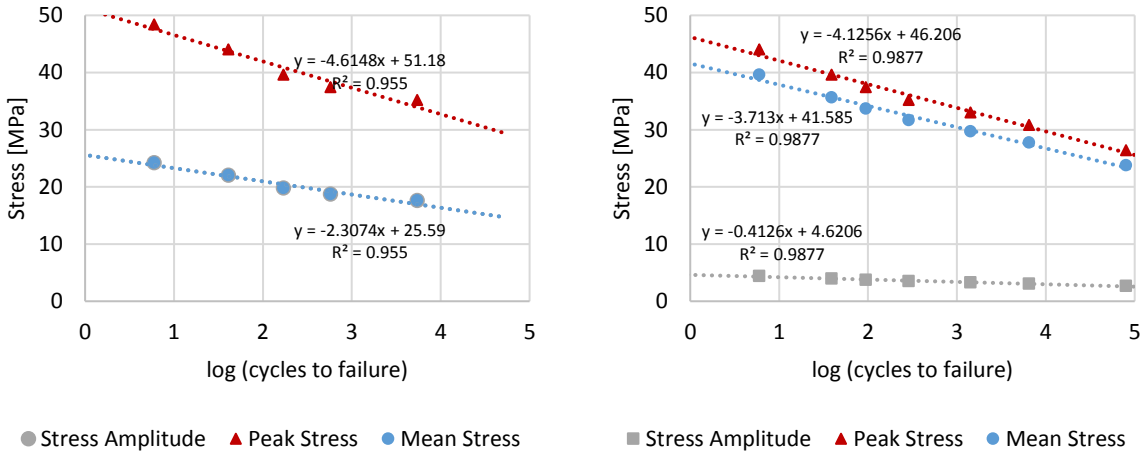

Figure 3: Plots of peak stress, mean stress, and stress amplitude against log(N) for loading ratios of [left] R=0 and [right] R=0.8

This fitting procedure was performed for all six loading ratios. Using these relationships, mean stress and stress amplitude parameters were estimated for various fatigue lives, and plotted as a Goodman diagram in Fig. 4.

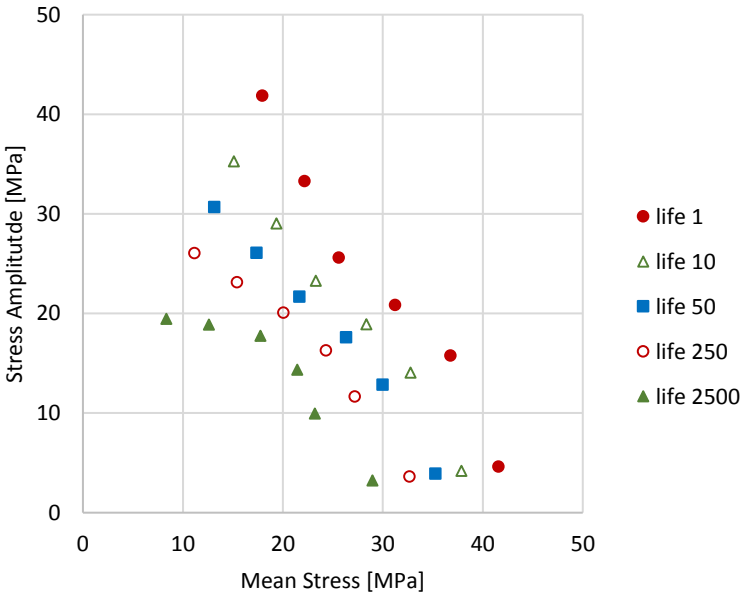

Figure 4: Goodman diagram based on fitting of experimental data

3.4 Relationships between dynamic performance and test parameters

The parameters collected for start, mid-life and penultimate cycle (Tables 2 and 3), were plotted against mean stress and amplitude. Certain clear and obvious relationships were present, as expected, cyclic strain values mapping linearly with cyclic stresses. As illustrated by Fig. 5, mid-life and final strains increased from the start of the test; this is consistent with the majority of fatigue behaviour observed, during which the material experiences increasing deformation as damage accumulates.
More notable is the effect observed when examining the ratio between initial and mid-life dynamic characteristics, in relation to the fatigue loading, as shown in Fig. 6. Although there is a loose correlation with stress amplitude for both loss tangent and dynamic stiffness ratios, both parameters come into a much tighter fit with mean stress. Fig. 7 shows the correlation of these parameters with loading ratio.

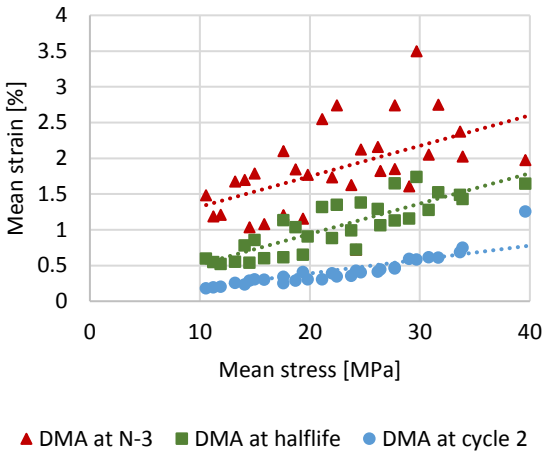

Figure 5: Mean strain plotted against mean stress at start, half-life, and end of test.

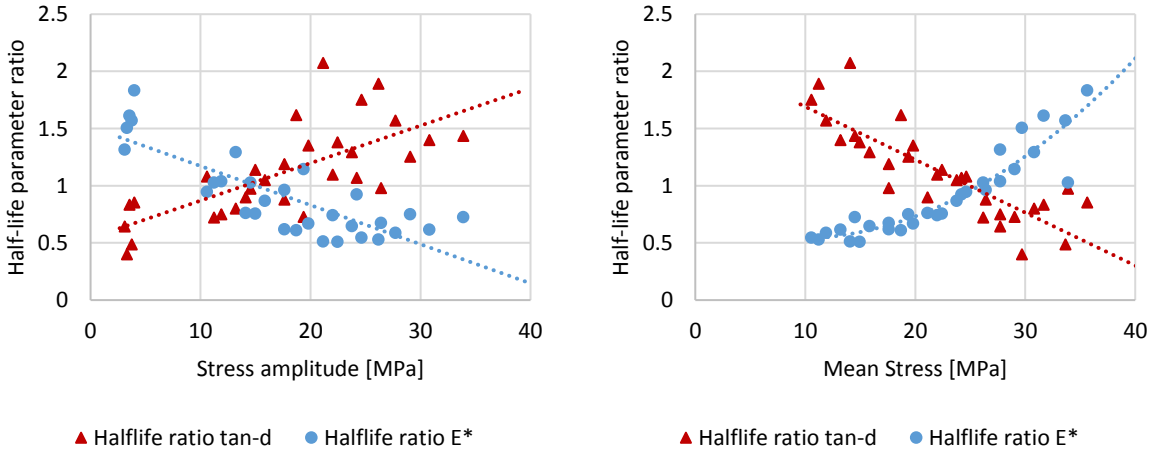

Figure 6: Ratio of half-life/initial values of dynamic stiffness and loss tangent plotted against [left] stress amplitude, [right] mean stress.

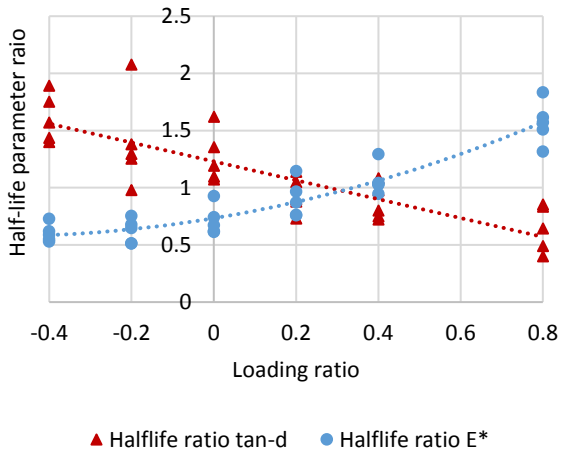

Figure 7: Ratio of half-life/initial values of dynamic stiffness and loss tangent plotted against loading ratio

4 DISCUSSION

It is moderately likely that the correct fitting of data such as those given in Fig. 3 would be either a curve, or two linear regions (as per Coffin-Manson and Basquin lines for metals [4-6]). However, on the basis of this small dataset, it is inconclusive, and a single linear fit appears adequate for the data available. As a minimum, this will be investigated by performing more tests at lower stress levels, to provide more data points and a more confident fitting.

The current approach is simple and pragmatic (as all the early work on metals fatigue) on the basis that for the target engineering applications, applied force on components will govern design rather than displacement. This is the approach taken by Basquin's law [6], but it assumes that the design aim is to achieve very long fatigue life, by remaining in the purely linear-elastic strain regime. Such an approach has been widely used with some success in studies of continuous fibre reinforced composites [7-11] From an engineering perspective, then there is no great concern with using this as an empirical solution, provided that the model is effective. However, in terms of materials science, it might reasonably be argued that this is not ideal, when working with a family of materials for which there is effectively no linear-elastic loading region under normal operating conditions. The use of strain-controlled tests is largely ineffective with continuous fibre composites, due to the effects of highly variable failure strain. However, with the more homogenous nature of injection moulded composites, using constant cyclic strain (as opposed to stress) levels may be a more insightful way to investigate their fatigue behaviour. This can present challenges for obtaining control measurements without affecting the specimen (due to the knife-edge contact for "clip-on" extensometers), but current best-in-class video extensometry provides sufficiently high bandwidth (readings per second) and low latency (time lag between camera frame and change in reading) that direct non-contact strain control is a feasible option (as demonstrated by the author last year [12]).

Examining Fig. 4, it seems clear that the simple approach used by the Goodman line would not be appropriate. Estimating the iso-life lines on the basis of monotonic strength, by drawing a chord between the same value on mean stress and amplitude axes, is clearly very conservative. Alternatively, extrapolating to significantly negative loading ratios (ie. towards fully reversed stress) on the basis of tension-tension fatigue data, will lead to significant over-estimation of the material's resistance to fatigue in that regime. It looks more probable that the use of a Gerber parabola [13] would be more suitable.

The changes in loss tangent and dynamic stiffness during the test are, of themselves, not surprising, but the relationship with mean stress observed in Fig. 6 is more so. Considering the ratio of initial loss tangent to mid-life value, then in this set of observations the loss tangent decreases during the test at

high mean stress, but increases with low mean stress. The relationship with mean stress appears linear, with the cross-over point lying at approximately half the peak stress sustained in monotonic test. By contrast, the change in dynamic stiffness during tests occurs in exactly the opposite sense, and the relationship with mean stress is not linear.

The implication of this is that when the fatigue stress drops to a minimum of zero, or is partially reversing, then stiffness decreases during the test and damping increases; this appears to meet the conventional expectations of fatigue behaviour in composites [14, 15].

Meanwhile in tests where there is a significant tensile static load underlying the alternating stress, the material appears to stiffen noticeably during early cycles and damping is reduced; this is less expected, but it has some congruence with behaviour observed in metals which experience strain hardening. Many thermoplastics can be drawn to enhance their properties, in terms of higher modulus and more linear behaviour. Hypothetically, the observed effect might be explained by an effect of creep drawing, causing more rapid increase in dynamic stiffness than the degradation caused by low amplitude fatigue.

5 CONCLUSIONS

This small study suggests that there is good potential to use the Goodman diagram as an analytical approach to developing a model of durability of injection moulding composites. From this initial study alone, there is insufficient evidence to support a specific model for the topography of the chart, so practical use for input to finite element models for design would rely upon much larger sample size (2x to 5x the number of specimens, or more).

The use of direct strain measurement was shown to provide interesting data, which could be used to gain further insight into the evolution of mechanical behaviour during the fatigue process. For this material, there appears to be a relationship between mean stress and change in stiffness during the life of the specimen, with relatively low scatter.

REFERENCES

[1] Goodman, J., *Mechanics Applied to Engineering*, Longmans Green and Company, London, 1899.

[2] Haigh, B. P. Experiments on the fatigue of brasses, *Journal of the Institute of Metals*, **18**, 1917, pp 55-86.

[3] Soderberg C.R., Factor of safety and working stress, *Transactions of the American Society of Mechanical Engineers*, **52**, 1930, pp 13-28.

[4] Coffin L.F., A study of the effects of cyclic thermal stresses on a ductile metal, *ASTM Transactions*, **76**, 1956, pp 931-950.

[5] Manson, S.S., Behaviour of materials under conditions of thermal stress, *Heat Transfer Symposium*, University of Michigan Engineering Research Institute, 1953, pp 9-75.

[6] Basquin, O.H., The Exponential Law of Endurance Tests, *ASTM Proceedings*, **10**, 1910, pp 625-630.

[7] Nijssen R.L.P., Cormier L., *Experiments and modeling of influence and interaction of temperature and frequency on fatigue life (Project UpWind deliverable D3.1.8 for European FP6 project No.019945*) Knowledge Centre for Wind Turbine Materials and Construction, Kluisgat 5, 1771MV Wieringerwerf, The Netherlands. 2010

[8] P.B.S Bailey, C. Hoehl, P. Jamshidi, C. Cowan, S. Squires, A. J. Smith. Enhanced fatigue testing of composites. *Proceedings of the 19th International Conference on Composite Materials*. 2013

[9] De Baere I., Van Paepegema W., Quaresimin M., Degrieck J.: On the tension–tension fatigue behaviour of a carbon reinforced thermoplastic Part II: Evaluation of a dumbbell-shaped specimen. *Polymer Testing*, **30**, p663-672, (2011).

[10] Xiao J., Bathias C.: Fatigue behaviour of unnotched and notched composite laminates. Composites Science and Technology, Vol. 50, p141-148, (1994).

[11] Pandita S.D., Huysmans G., Wevers M., Verpoest I., Tensile fatigue behaviour of plain weave fabric composites in on- and off-axis directions, *Composites: Part A*, **32,** 2001, pp 1533-1539.

[12] Bailey P.B.S., Higham M., Application of strain-controlled fatigue testing methods to polymer matrix composites, *Procedia Structural Integrity*, **2**, 2016, pp 128-135

[13] Gerber, W.Z., [Relation between the superior and inferior stresses of a cycle of limiting stress] (in German), *Zeitschrift des Bayerischen Architekten und Ingenieur-Vereins*, **6**, 1874, pp 101-110.

[14] ISO 13003:2003, *Fibre-reinforced plastics - determination of fatigue properties under cyclic loading conditions*, ISO 2003.

[15] ASTM D 3479 / D 3479M – 12, *Standard test method for tension-tension fatigue of polymer matrix composite materials*. ASTM 2012